THESIS FOR THE DEGREE OF DOCTOR OF PHILOSOPHY IN SOLID AND STRUCTURAL MECHANICS

On integral equation methods of solution to eddy current interaction problems

LARS LARSSON

Department of Applied Mechanics
CHALMERS UNIVERSITY OF TECHNOLOGY
Göteborg, Sweden 2014

On integral equation methods of solution to eddy current interaction problems
LARS LARSSON
ISBN 978-91-7597-045-5

© LARS LARSSON, 2014

Doktorsavhandlingar vid Chalmers tekniska högskola
Ny serie nr. 3726
ISSN 0346-718X
Department of Applied Mechanics
Chalmers University of Technology
SE-412 96 Göteborg
Sweden
Telephone: +46 (0)31-772 1000

Chalmers Reproservice
Göteborg, Sweden 2014

On integral equation methods of solution to eddy current interaction problems
Thesis for the degree of Doctor of Philosophy in Solid and Structural Mechanics
LARS LARSSON
Department of Applied Mechanics
Chalmers University of Technology

Abstract

The eddy current method is used for nondestructive evaluation of conducting materials. To achieve a greater knowledge and insure safe and reliable evaluation methods, the use of mathematical models and simulations are needed. In this thesis integral equation methods of solutions are applied to solve the eddy current interaction problem which essentially is a scattering problem. This involves a Green's function technique to generate integral relations between the surface fields and the fields everywhere else. Then the key is to use suitable basis functions to describe the surface fields. In the end numerical integration is used to obtain the solution, the change of impedance due to the scatterer. The scatterer in this case is a model of a defect and the source is a single conductor or a single coil. The solutions are compared to Finite Element solutions with good agreement.

This thesis includes four papers where two different methods of solution have been used. In the first paper, the T matrix method is applied on a 2D problem with a subsurface defect. The second paper presents a boundary integral equation method solution to a problem with a surface-breaking flat and infinitely long crack. In the third and fourth papers the 3D problem of a rectangular crack is solved also using a boundary integral method. In the third paper the surface of the material is a plane and in the fourth it is the inside of a cylindrical hole.

All papers contain comparisons with finite elements calculations and good agreement is found for all methods presented in the present thesis. The advantage of these methods compared with the finite element method is the numerical efficiency.

Keywords: Nondestructive evaluation, Scattering, Eddy current, T matrix, Boundary integral equation

Preface

The work of the three first year of my doctoral studies was part of the European project "PICASSO" and the funding from the European Commission within the FP7 programme is gratefully acknowledged.

The completion of this thesis is credited the following persons: my supervisor Anders Boström, my co-supervisors Peter Bövik and Håkan Wirdelius and my roommate Anders Rosell who also has been a member of the "PICASSO" project, all of them also being co-authors.

I thank my supervisor Anders Boström for his excellent guidance. I also would like to thank all of my colleges in the Advanced NDT group for making the duration of this work a pleasant time. Finally I would like to thank my family and friends for all support and happy moments. I especially express my deepest gratitude to my fiancée Helena and our daughter Linnéa, for all support, encouragement and happiness. You have given me the strength to make this possible.

Lars Larsson
June 2014

Thesis

This thesis consists of an extended summary and the following appended papers:

Paper A L. Larsson and A. Rosell. "The T matrix method for a 2D eddy current interaction problem". *AIP Conf. proc. Reveiw of progress in quantitative nondestructive evaluation.* Vol. 1430. Burlington, Vermont, 2012, pp. 316–323

Paper B L. Larsson, A. Boström, P. Bövik, and H. Wirdelius. Integral equation method for eddy current nondestructive evaluation of a tilted, surface-breaking crack. *J. Appl. Phys.* **114** (2013), 194504 –194504–6

Paper C L. Larsson. Integral equation method for evaluation of eddy-current impedance of a tilted, rectangular, surface-breaking crack. *To be submited for international publication.* (2014)

Paper D L. Larsson and A. Boström. Integral equation method for evaluation of eddy-current impedance of a rectangular, near surface crack inside a cylindrical hole. *To be submited for international publication.* (2014)

Three of the papers are written with co-authors. In the first paper the author of this thesis has preformed all of the work except the finite element calculations. In the second paper the author of this thesis has carried out a large part of the derivations, all the numerical implementations and written parts of the paper. In paper D the author of this thesis was responsible for the major progress of work.

Contents

Extended Summary

The subject of this thesis is methods of solution for eddy-current nondestructive evaluation using integral equation methods. The ambition is to apply methods that have successfully been used on the elastodynamic scattering problem to the electromagnetic scattering problem.

1 Introduction

1.1 Background and motivation

Nondestructive evaluation (NDE) methods are used to insure the quality of safety-critical components, e.g. turbine blades in a jet-engine. One of these methods is the eddy current method which is used for nondestructive evaluation of conductive materials. Eddy currents are generated by applying an alternating current to a small coil positioned near the surface of the material. A crack will interfere with the currents and in that way affect the impedance of the coil. By measuring this impedance, cracks can be found. When an aircraft engine is constructed it is designed to withstand loads higher than it ever will be affected of during operation. Even so the aging engine will eventually degrade to a state where its structural design becomes too weak. Therefore it is of great importance to observe this degradation and take the engine out of use before that moment. This observation is carried out by use of different NDE methods. To ensure a reliable result of the inspection, specific testing procedures are developed for every different part that is to be tested. In the development of these procedures the probability of detection (POD) methodology is an important instrument (see for example [8], [23] and [21]). The POD is a tool that is used to ensure a method's capability in an NDE application. The POD curve shows the estimated probability to detect a defect as a function of different parameters, e.g. defect size. These curves is most often produced by an expensive experimental procedure, where lots of different defects are to be fabricated into the test pieces. To obtain the POD curves by use of simulations is therefore very desirable.

In the field of nondestructive testing and evaluation, mathematical models are important tools to secure the safety and reliability of the testing methods. With these models simulations of the testing processes can be done to achieve a greater knowledge of the process. Of special interest is the use of statistical models together with the mathematical model to estimate the probability of detection (POD). There are great advantages with using a mathematical model to predict the signal from the nondestructive testing instrument due to a crack. In the model the defect parameters can be varied in an infinite range, while a specific defect when manufactured can often be very difficult to retrieve.

1.2 Eddy current nondestructive testing

The eddy current method is an electromagnetic method. The testing instrument, a probe containing a coil is emitting electromagnetic waves. The resulting electromagnetic field induces eddy currents in the material below the probe. Therefore the evaluated material has to be conductive, even if the conductivity may be low. Due to the nature of induction the eddy currents are exponentially decreasing into the depth of the material, therefore the method is mostly used to detect surface breaking or near surface defects. How fast the fields will decay is dependent of the frequency of the input current which is the same as the frequency of the involved fields. In applications of eddy current testing the typical range of the frequency is a few kHz to several MHz. A lower frequency field penetrates deeper into the material, but it also contains less energy compared to a field of higher frequency and therefore generates a weaker signal. The method can also be used to measure or detect other things than cracks that are influencing the impedance, for example hardness, thickness of the material or presence of corrosion.

There are several parameters of the probe that affects the output of the eddy current testing such as presence of shields and ferrite cores to focus the field towards the inspected material. In the present thesis such parameters are not included and the probe are modelled as a single conductor or coil to obtain an analytical expression of the incoming field transmitted from the probe. The parameters of the defect that have an influence on the change in impedance are for example depth and subsurface position, size and tilt of the defect. In papers A and D the defects are near surface and the subsurface position has a clear influence of the change in impedance. The parameter of depth or height of the defect is included in all of the papers. The defect in paper B is an infinitely long, flat, surface-breaking and tilted crack. The length of the defect can be varied in papers C and D where the cracks are rectangular.

1.3 Simulation methods

The finite element method (FEM) and boundary element methods (BEM) are commonly used in eddy-current simulations, see for example [19] or [10]. In situations with complex geometry, either of the defect or probe, FEM is very suitable. In the case of homogeneous and isotropic material BEM can be used as an alternative. In BEM the dimensionality of the problem is reduced, by use of the Green's tensor, into integral equations on the boundary. The computational efficiency of BEM is dependent on how fast the expression of the Green's tensor can be generated. By combining the Discrete Complex Image Method (DCIM) with the method of the Generalized Pencil of Function (GPOF) this can be done with a very high computational efficiency [22]. Analytical expressions are usually used for the incoming field such as presented in [5] for the field from a single coil close to a conducting half space or in [4] for the field from a single coil positioned inside of a cylindrical hole in a conductor. Analytical expressions also exists for the field from a single coil with the presence of a ferrite core [24]. In BEM the fields at the boundaries are discretized by similar methods as in FEM. In addition to FEM and BEM there exists several methods for simulation of eddy current including thin-skin approximations, eg.

[17], methods using the Wiener-Hopf technique [7], and methods based on geometrical theory of diffraction [6]. With the concept of model assisted probability of detection (MaPOD) see e.g. Jensen et al. [8], Wirdelius and Persson [23], and Rosell and Persson [21], where a large number of simulations are needed, the demand of efficient numerical methods has increased.

2 Electromagnetic and Elastodynamic fields

2.1 Electromagnetic fields

The eddy current method is an electromagnetic method and the electromagnetic fields are obeying Maxwell's equations (see [18])

$$\nabla \cdot \left(\varepsilon^{-1}\boldsymbol{E}\right) = \rho \tag{2.1}$$

$$\nabla \cdot \boldsymbol{B} = 0 \tag{2.2}$$

$$\nabla \times \boldsymbol{E} = -\frac{\partial \boldsymbol{B}}{\partial t} \tag{2.3}$$

$$\nabla \times \left(\mu^{-1}\boldsymbol{B}\right) = \boldsymbol{J} + \frac{\partial(\varepsilon \boldsymbol{E})}{\partial t} \tag{2.4}$$

The presentation in this elegant form simplifies the interpretation of the equations. The electric field $\boldsymbol{E}$ is created by charges (ρ) and the magnetic field $\boldsymbol{B}$ by moving charges, the current $\boldsymbol{J}$. Equations (2.3) and (2.4) also imply that a change of the magnetic field produces an electric field and vice versa. The material is assumed to be homogeneous, isotropic and linear, then the electric permittivity ε and the magnetic permeability μ are constants. When seeking a solution, it is preferable to reformulate Eqs. (2.1) – (2.4) in order to get fewer equations to work with. This can be done by taking the curl of Eq. (2.3) and substituting the obtained right hand side by use of Eq. (2.4). Equation (2.2) implicates that the magnetic field $\boldsymbol{B}$ can be expressed as the curl of a magnetic vector potential $\boldsymbol{A}$, $\boldsymbol{B} = \nabla \times \boldsymbol{A}$. Inserting this in Eq. (2.3) gives

$$\nabla \times (\boldsymbol{E} + \frac{\partial \boldsymbol{A}}{\partial t}) = 0 \tag{2.5}$$

and the expression of $\boldsymbol{E}$ in terms of potentials become

$$\boldsymbol{E} = -\nabla V - \frac{\partial \boldsymbol{A}}{\partial t}, \tag{2.6}$$

where V is a scalar function. The potentials are not unique by these definitions and can be changed without affecting $\boldsymbol{E}$ or $\boldsymbol{B}$. Here it is possible to chose a gauge such that ∇V is eliminated, then Eq. (2.4) can be written as

$$\nabla \times \nabla \times \boldsymbol{A} = \mu_0 \boldsymbol{J} - \mu_0 \varepsilon_0 \frac{\partial^2 \boldsymbol{A}}{\partial t^2}. \tag{2.7}$$

The currents appear in form of source currents and conductive currents, $\boldsymbol{J} = \boldsymbol{J}_s + \sigma \boldsymbol{E}$, where σ is the conductivity. Further on, $\boldsymbol{E}$ is assumed to have zero divergence ($\rho = 0$) meaning that there only exists closed currents, being the case for all field problems presented in the present thesis. By use of this, together with the vector identity $\nabla \times \nabla \times \boldsymbol{A} = \nabla(\nabla \cdot \boldsymbol{A}) - \nabla^2 \boldsymbol{A}$ in Eq. (2.7), gives (the harmonic time factor $\mathrm{e}^{-\mathrm{i}\omega t}$ is assumed throughout this thesis)

$$\nabla^2 \boldsymbol{A} + k^2 \boldsymbol{A} = -\mu_0 \boldsymbol{J}_s, \tag{2.8}$$

where $k^2 = i\mu\omega\sigma + \omega^2\mu\varepsilon$. Equation (2.8) together with the radiation condition at infinity and different boundary conditions is the mathematical model that is used in this thesis to solve the eddy current interaction problem. The equation is called Helmholtz equation and it does not only describe eddy current interaction problems but also other scattering problems.

For a boundary between two regions $i = 0$ and $i = 1$ the magnetic vector potential $\boldsymbol{A}_i$ satisfies the following condition

$$\hat{n} \times \boldsymbol{A}_0 = \hat{n} \times \boldsymbol{A}_1, \tag{2.9}$$

$$\frac{1}{\mu_0} \hat{n} \times (\nabla \times \boldsymbol{A}_0) = \frac{1}{\mu_1} \hat{n} \times (\nabla \times \boldsymbol{A}_1), \tag{2.10}$$

where $\hat{n}$ is the unit vector perpendicular to the boundary. The boundary condition taken across a crack is given below by Eqs. (3.4) and (3.5).

2.2 Elastodynamic fields

To state the reason why the same methods of solution can be used on the elastodynamic and the electromagnetic scattering problems, this section is given to throw light upon the unity in the mathematical nature of both types of fields. For a time harmonic elastodynamic field the displacement $\boldsymbol{u}$ satisfies

$$(\lambda + 2\mu)\nabla(\nabla \cdot \boldsymbol{u}) - \mu \nabla \times (\nabla \times \boldsymbol{u}) + \boldsymbol{f} = -\omega^2 \rho \boldsymbol{u}, \tag{2.11}$$

where μ and λ are called Lamé constants and $\boldsymbol{f}$ is the body force. This equation can be rewritten by introducing the Helmholtz decomposition of $\boldsymbol{u}$

$$\boldsymbol{u} = \nabla\phi + \nabla \times \boldsymbol{\psi}, \tag{2.12}$$

where $\nabla \cdot \boldsymbol{\psi} = 0$. Here ϕ and $\boldsymbol{\psi}$ are scalar and vector potentials of the displacement field. Substituting $\boldsymbol{u}$ in Eq. (2.11) with Eq.(2.12) yields

$$(\nabla^2 + \frac{\omega^2}{c_p^2})\phi = f_p, \tag{2.13}$$

$$(\nabla^2 + \frac{\omega^2}{c_s^2})\boldsymbol{\psi} = \boldsymbol{f}_s, \tag{2.14}$$

where $\boldsymbol{f} = (\lambda + 2\mu)\nabla f_p + \mu\nabla \times \boldsymbol{f}_s$ and $\nabla \cdot \boldsymbol{f}_s = 0$. Here $c_p = \sqrt{(\lambda + 2\mu)/\rho}$ and $c_s = \sqrt{\mu/\rho}$ are the wave speeds of the pressure and shear waves respectively. Both the scalar and vector potentials of the displacement field and the magnetic vector potential are satisfying Helmholtz equation. Because of that the behavior of the elastodynamic and electromagnetic fields in an infinite continuum are similar, but at a boundary Eq. (2.13) and (2.14) are in general coupled. Either way the similarities between the different fields do motivate the use of the same methods of solution for both of the field problems.

3 The methods of solution

An efficient way of discretization is a key ingredient to gain an efficient numerical method of solution. For some simple crack geometries the boundary integral equations can be discretized using specific basis functions suitable to the geometry of interest. This approach is used in the present thesis, for a strip-like crack in paper B and a rectangular crack in paper C and D. In paper A the T matrix method, which successfully have been used to solve other scattering problems (see for example Refs. [9], [11], [12]) is applied to a 2D eddy current scattering problem. By use of this method a transition matrix is calculated which then can be used together with the incoming field to give the change in impedance. Just like FEM and BEM the methods in this thesis provide accurate results for incoming fields of arbitrary frequencies in the typical range for eddy current applications.

3.1 The integral representation

The methods in this thesis make use of a Green's function technique to get an integral representation of the problem. This integral representation expresses the fields everywhere in terms of the fields on the boundaries. In this way the dimensionality of the problem is reduced to the determination of surface fields. The Green's function $G(\boldsymbol{r}, \boldsymbol{r}\,', k)$ to equation (2.8) satisfies

$$\nabla^2 G(\boldsymbol{r}, \boldsymbol{r}\,', k) + k^2 G(\boldsymbol{r}, \boldsymbol{r}\,', k) = -\delta(\boldsymbol{r} - \boldsymbol{r}\,'), \tag{3.1}$$

together with the radiation condition at infinity. Here $\delta(\boldsymbol{r} - \boldsymbol{r}\,')$ is the 3D Dirac delta function. In other words the Green's function is the solution to the differential equation for a point source. To illustrate how the Green's function technique is used to solve Helmholtz equation the procedure for deriving the integral representation for a general scattering case is now given. Beginning with multiplication of equation (2.8) with $G(\boldsymbol{r}, \boldsymbol{r}\,', k)$ and subtracting equation (3.1) multiplied with $\boldsymbol{A}(\boldsymbol{r})$ yields

$$G(\boldsymbol{r}, \boldsymbol{r}\,', k)\nabla^2 \boldsymbol{A}(\boldsymbol{r}) - \boldsymbol{A}(\boldsymbol{r})\nabla^2 G(\boldsymbol{r}, \boldsymbol{r}\,', k) + \mu_0 \boldsymbol{J}_s G(\boldsymbol{r}, \boldsymbol{r}\,', k) = \boldsymbol{A}(\boldsymbol{r})\delta(\boldsymbol{r} - \boldsymbol{r}\,'). \tag{3.2}$$

Now the scattering geometry described by figure 3.1 is considered. The source is positioned inside the surface S_i and the scatterer is bounded by the surface S_{sc}. Continuing with

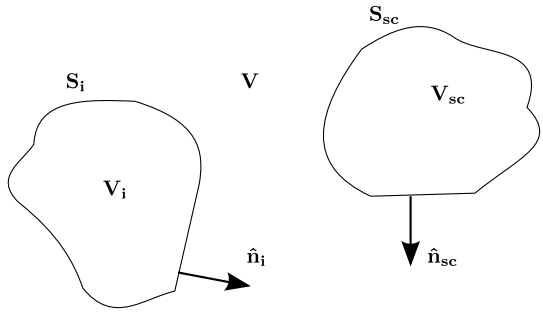

Figure 3.1: *Scattering geometry*

integration of equation (3.2) over the volume V (all space outside S_i and S_{sc}) and using Green's theorem gives

$$
\begin{aligned}
-\int_{S_{sc}} \Big(\big((\nabla \cdot \boldsymbol{A}(\boldsymbol{r}))\hat{\boldsymbol{n}}_{sc} - \hat{\boldsymbol{n}}_{sc} \times (\nabla \times \boldsymbol{A}(\boldsymbol{r})) \big) G(\boldsymbol{r}, \boldsymbol{r}\,', k) \\
-(\hat{\boldsymbol{n}}_{sc} \cdot \boldsymbol{A}(\boldsymbol{r}))\nabla G(\boldsymbol{r}, \boldsymbol{r}\,', k) - (\hat{\boldsymbol{n}}_{sc} \times \boldsymbol{A}(\boldsymbol{r})) \times \nabla G(\boldsymbol{r}, \boldsymbol{r}\,', k) \Big) \, \mathrm{d}S_{sc} \\
+ \boldsymbol{A}^{in}(\boldsymbol{r}') = \begin{cases} \boldsymbol{A}(\boldsymbol{r}') & \boldsymbol{r}' \text{ outside } S_{sc}, \\ 0 & \boldsymbol{r}' \text{ inside } S_{sc}, \end{cases}
\end{aligned}
\tag{3.3}
$$

where $\boldsymbol{n}_{sc}$ is the outward normal to the surface of the scatterer and $\boldsymbol{A}^{in}(\boldsymbol{r}')$ is the incoming field obtained by integrating the third term in Eq. (3.2) (see Eq. (3.10) below). The first row in the integral representation (3.3) is used in integral equation methods while the T matrix method also makes use of the second row.

In eddy current interaction there only exist closed currents and $\nabla \cdot \boldsymbol{E}(\boldsymbol{r}) = 0$. In paper A where the 2D case is considered the third term in the surface integral in Eq. (3.3) is also zero as $\hat{\boldsymbol{n}}_{sc} \cdot \boldsymbol{A}(\boldsymbol{r}) = 0$. The other terms will remain, but in a much simpler form. In papers B, C and D the scatterer is a flat crack where the boundary condition across the crack are taken as

$$
\nabla \times \boldsymbol{A}(\boldsymbol{r})_- = \nabla \times \boldsymbol{A}(\boldsymbol{r})_+, \tag{3.4}
$$

$$
\hat{\boldsymbol{n}}_{sc} \cdot \boldsymbol{A}(\boldsymbol{r})_- = \hat{\boldsymbol{n}}_{sc} \cdot \boldsymbol{A}(\boldsymbol{r})_+ = 0. \tag{3.5}
$$

Here the indices plus and minus denote the limit from the two sides. By introducing these boundary conditions the surface integral is reduced to only contain the last term. The resulting integral representation seems to be neat, but an even more convenient integral representation for this case can be found by using another form of Green's theorem and the Green's tensor of the metal (see Bowler [3])

$$
\hat{\boldsymbol{x}} \cdot \boldsymbol{A}^{in}(\boldsymbol{r}') + i\omega \lim_{x \to 0^+} \int_{-b/2}^{b/2} \int_0^a G_{xx}(\boldsymbol{r}, \boldsymbol{r}') V(\boldsymbol{r}') \, \mathrm{d}z' \mathrm{d}y' = 0, \tag{3.6}
$$

where the x axis is perpendicular to the surface of the crack and G_{xx} is the xx component of the tensor. Here $\nabla' V(\boldsymbol{r'}) = \boldsymbol{E}^-(\boldsymbol{r'}) - \boldsymbol{E}^+(\boldsymbol{r'})$ is the jump in the electric field across the crack. The crack lies in the yz-plane and has the height a and length b. This integral representation is used in papers B, C and D.

3.2 The probe

In addition to the formulation of the integral representations (3.3) and (3.6), Green's theorem is also of great importance in the calculation of the impedance. The change in coil impedance due to a crack can be calculated by the following integration over a surface enclosing the coil (see [1])

$$\Delta Z = \frac{1}{I^2} \int_{S_i} (\boldsymbol{E}_b \times \boldsymbol{H}_a - \boldsymbol{E}_a \times \boldsymbol{H}_b) \cdot \boldsymbol{n} \, \mathrm{d}S. \tag{3.7}$$

With the index b denoting the fields in the presence of a defect and a the fields in the absence of a defect. Again the calculation only involves surface fields. Now by use of Green's theorem and Lorentz reciprocity relation for a source-free region

$$\nabla \cdot (\boldsymbol{E}_a \times \boldsymbol{H}_b - \boldsymbol{E}_b \times \boldsymbol{H}_a) = 0, \tag{3.8}$$

Eq. (3.7) can be rewritten in an even more convenient form

$$\Delta Z = \frac{1}{I^2} \int_{S_{sc}} (\boldsymbol{E}_a \times \boldsymbol{H}_b - \boldsymbol{E}_b \times \boldsymbol{H}_a) \cdot \boldsymbol{n} \, \mathrm{d}S. \tag{3.9}$$

Here the integration is over a surface enclosing the defect. The information about the coil geometry is now needed only to determine the incoming field. Thus it is possible to derive an expression for the change in impedance due to a specific scatterer for an arbitrary source.

The geometry of the transmitting source is most often simple and in the present thesis analytical expressions are used for the incoming fields. The field in the air originating from the probe can be expressed as

$$\boldsymbol{A}^{in}(\boldsymbol{r'}) = \int_{V_i} \mu_0 \, \boldsymbol{J}_s(\boldsymbol{r}) G(\boldsymbol{r}, \boldsymbol{r}\,', k) \mathrm{d}V, \tag{3.10}$$

where $G(\boldsymbol{r}, \boldsymbol{r}\,', k)$ is the scalar free space Green's function and $\boldsymbol{J}_s$ the current density of the source current. In paper A where the integral equations are for the whole geometry this expression is used without any alteration. In paper B, C and D the integral equations are over the crack only and the expression needs to be transformed to give the incoming field in the metal below the probe by use of the transmission coefficients of the boundary between the air and metal. The incoming field used in paper B and C is given by Dodd and Deeds in [5] and the incoming field from the probe inside the cylindrical hole in paper D is given by Burke and Theodoulidis in [4].

3.3 Basis functions

A set of functions is called a basis if every solution can be expressed as a sum of these functions. The functions in such a set are called basis functions. It is a great advantage to expand the unknown solution in such known functions and the technique is used in many methods of solution. Then the problem consists of determining the expansion coefficients.

In this section some of the basis functions used in the present thesis are given and some of their important properties are pointed out.

3.3.1 In 2D

The solution to Helmholtz equation (2.8) in 2D on a cylindrical surface can be expanded as

$$A(r,\theta) = \sum_{m\varsigma} \zeta_{m\varsigma} Re\chi_{m\varsigma}(\boldsymbol{r}, k), \tag{3.11}$$

where $\zeta_{m\varsigma}$ are the unknown expansion coefficients and the basis are defined as

$$Re\chi_{m\varsigma}(\boldsymbol{r}, k) = \frac{\sqrt{\epsilon_m}}{2} J_m(kr) \begin{cases} \cos(m\phi), & \text{if}\, \varsigma = e, \\ \sin(m\phi), & \text{if}\, \varsigma = o. \end{cases} \tag{3.12}$$

Here $J_m(kr)$ is a Bessel function, $m \in N$ and ς denotes odd or even.

The solutions can also be expressed in terms of plane waves which are convenient when the scattering surface is a plane, e.g. the surface of the conductive material. By expanding the solution in plane waves it becomes easier to interpret how the frequency of the fields and the electrical and magnetic properties of the material (σ, μ and ε) affect the solution. The plane wave basis functions are defined as

$$\varphi(\boldsymbol{k}, \boldsymbol{r}) = \frac{1}{\sqrt{8\pi}} e^{i\boldsymbol{k}\cdot\boldsymbol{r}}, \tag{3.13}$$

where $\boldsymbol{k} = k\hat{\boldsymbol{k}}$. Here $\hat{\boldsymbol{k}}$ is the unit vector in the direction of propagation. The imaginary part of k affects the amplitude whereas the real part affects the phase. In the eddy current interaction problem the frequency is assumed to be low such that $\sigma \gg \omega\,\varepsilon$. Because of this the imaginary part is equal to the real part, i.e. $k = (1+i)\sqrt{\mu\,\omega\,\sigma/2}$. This states that the important parameter is the product $\mu\,\omega\,\sigma$ and justifies the introduction of the variable $\delta = \sqrt{2/\mu\,\omega\,\sigma}$ which is a length and is called the skin depth. At one skin depth the amplitude of the field has been reduced to 37% (e^{-1}) of the amplitude at the surface.

3.3.2 In 3D

In 3D the electromagnetic vector field is conveniently expanded in vector basis functions which except being solutions to Helmholtz equation also share other properties with the

electromagnetic field. In paper D the following cylindrical vector basis functions are used

$$\begin{aligned}\chi^j_{1m}(h,\boldsymbol{r}) &= \frac{1}{q_j\sqrt{8\pi}}\nabla\times(\hat{z}H^{(1)}_m(q_jr)e^{im\phi}e^{ihz}),\\ \chi^j_{2m}(h,\boldsymbol{r}) &= \frac{1}{k_jq_j\sqrt{8\pi}}\nabla\times\nabla\times(\hat{z}H^{(1)}_m(q_jr)e^{im\phi}e^{ihz}),\end{aligned} \tag{3.14}$$

where $q_j=\sqrt{k_j^2-h^2}$. Here $H^{(1)}_m$ is a Hankel function of the first kind. The relation between the two sets of basis functions are similar to the relation between the electric and magnetic fields

$$\begin{aligned}\chi_{1mj}(h,\boldsymbol{r}) &= \frac{1}{k_j}\nabla\times\chi^j_{2m}(h,\boldsymbol{r}),\\ \chi_{2mj}(h,\boldsymbol{r}) &= \frac{1}{k_j}\nabla\times\chi^j_{1m}(h,\boldsymbol{r}).\end{aligned} \tag{3.15}$$

Another advantage of using these basis functions are that the condition of solenoidal magnetic field Eq. (2.2) is automatically satisfied. A consequence of this is that also the electric field will be solenoidal when expanded in this basis which is suitable in source free regions. In paper D where the surface geometry is the inside of a cylindrical hole, the Green's tensor is expressed as an expansion in these basis functions

$$\boldsymbol{G}(\boldsymbol{r},\boldsymbol{r'})=\begin{cases} i\sum_{\tau m}\int_{-\infty}^{\infty}\big[Re\chi_{\tau m1}(h,\boldsymbol{r}_<)\chi^\dagger_{\tau m1}(h,\boldsymbol{r}_>) \\ \qquad +\sum_{\tau'}\chi_{\tau' m1}(h,\boldsymbol{r})R^m_{\tau'\tau}(h)\chi^\dagger_{\tau m1}(h,\boldsymbol{r'})\big]\mathrm{d}h & \text{in metal,} \\ i\sum_{\tau\tau' m}\int_{-\infty}^{\infty}Re\chi_{\tau' m0}(h,\boldsymbol{r})T^m_{\tau'\tau}(h)\chi^\dagger_{\tau m0}(h,\boldsymbol{r'})\mathrm{d}h & \text{in cylinder}\end{cases} \tag{3.16}$$

where $Re\chi_{\tau mj}$ are the regular counterparts to (3.14) with the Bessel functions instead of Hankel functions. Here the functions $\chi^\dagger_{\tau m1}$ have a sign change in the exponential containing z. The inside space of the cylindrical hole is denoted region $j=0$ and the surrounding metal as region $j=1$. The reflection and transmission coefficients, $R^m_{\tau'\tau}(h)$ and $T^m_{\tau'\tau}(h)$ are derived by use of the boundary conditions on the cylindrical surface

$$\hat{r}\times\boldsymbol{E}_0=\hat{r}\times\boldsymbol{E}_1, \tag{3.17}$$

$$\frac{1}{\mu_0}\hat{r}\times(\nabla\times\boldsymbol{E}_0)=\frac{1}{\mu_1}\hat{r}\times(\nabla\times\boldsymbol{E}_1), \tag{3.18}$$

which when applied to (3.16) gives

$$\begin{aligned}\hat{r}\times\big[Re\chi_{\tau m1}(h,\boldsymbol{r_c})+\sum_{\tau'}\chi_{\tau' m1}(h,\boldsymbol{r_c})R^m_{\tau'\tau}(h)\big]=& \\ \hat{r}\times\sum_{\tau'}Re\chi_{\tau' m0}(h,\boldsymbol{r_c})T^m_{\tau'\tau}(h),&\end{aligned} \tag{3.19}$$

$$\hat{r} \times \left[\nabla \times \left[Re\chi_{\tau m1}(h, \boldsymbol{r_c}) + \sum_{\tau'} \chi_{\tau' m1}(h, \boldsymbol{r_c}) R^m_{\tau'\tau}(h)\right]\right] = \hat{r} \times \left[\nabla \times \sum_{\tau'} Re\chi_{\tau' m0}(h, \boldsymbol{r_c}) T^m_{\tau'\tau}(h)\right]. \tag{3.20}$$

Here r_c is the radius of the cylindrical surface. Then using the relation (3.15) to discard the $\nabla\times$ operators in (3.20) a system of equations which is straightforward to solve is obtained.

The main difference of the methods in the present thesis compared to the finite element method (FEM) or the boundary element method (BEM) is the choice of basis functions. The basis functions above are preferably used to describe the field on a cylindrical or plane surface, respectively. In paper B, C and D basis functions related to the Chebyshev polynomials are used to expand the jump in the electric field over a strip-like or a rectangular crack. These basis functions posses the important quality to give the expansion the correct weak singularity at the crack edge [3]. Other basis functions can be used for other kind of surfaces. With BEM this is avoided by discritizing the surfaces into a set of elements. Then quite simple basis functions can be used e.g. a polynomial of low order. In FEM the Green's functions technique is not used at all and the entire volume of interest is discritized in a set of elements.

3.4 Numerical integration

All methods in the present thesis involves numerical integration. Because of the nature of the Green's tensor some of these integrals needs to be handled with care. The correct choice of basis functions resolves a great part of the difficulties, e.g. the discretization in Chebyshev polynomials is taking care of the hypersingularity in that integral equation. To obtain a reasonable convergence analytical expansions of the dominating terms are also used. In paper B and C the following integral is solved in this way

$$\int_{-\infty}^{\infty} \frac{s^2}{h} I_m(qa) I_{m'}(-qa)\,\mathrm{d}q, \tag{3.21}$$

where a is the height of the crack and

$$I_m(\gamma) = \int_0^1 \cos((2m-1)\arcsin t)\mathrm{e}^{\mathrm{i}\gamma t}\mathrm{d}t. \tag{3.22}$$

Here $h = \sqrt{k_0^2 - s^2}$, $s^2 = p^2 + q^2$ and both q and p are Fourier transform variables. The integrand in (3.21) is divergent, but when integrated together with the reflected part of the Green's tensor the leading order terms cancel. The remaining leading order terms of (3.21) for large arguments can be written as

$$\frac{\pi}{|2q|}((1-2m')J_{2m'}(qa) + (1-2m)J_{2m}(qa)) + \frac{\pi(-1)^{m'}(2m'-1)(-1)^m(2m-1)}{4aq^2}. \tag{3.23}$$

This is integrated analytically by use of

$$\int_0^\infty \frac{J_m(qa)}{q}\mathrm{d}q = \frac{1}{m}, \quad \text{for} \quad m = 1, 2, ... \tag{3.24}$$

to get reasonable convergence. In paper D the part that originates from the free space part of the Green's tensor

$$\int_{-\infty}^\infty \frac{s^2}{hp^2} J_n(pa/2) J_{n'}(-pa/2)\mathrm{d}p, \tag{3.25}$$

has to be integrated in a similar way, but in this case it is easier to identify the dominating term which can be integrated analytically by use of

$$\int_0^\infty \frac{1}{p} J_n(p) J_{n'}(p)\mathrm{d}p = \frac{\delta_{nn'}}{2n}, \quad \text{for even} \quad n + n', \tag{3.26}$$

The method of numerical integration used in this thesis is the Gauss-Legendre quadrature. It is an efficient method which also manages to deal with weak singularities.

4 Results

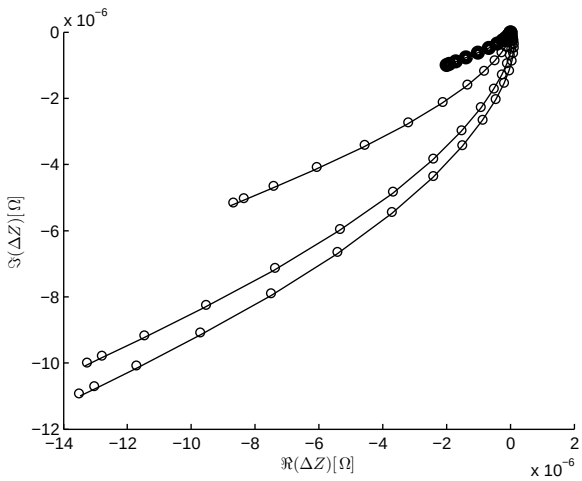

Figure 4.1: *The real versus the imaginary part of ΔZ during a surface scan. The lengths of the cracks are* 1 mm, 2 mm, 4 mm, 8 mm *and* 10 mm, *(starting from the top). The scanning is in the normal direction over the center of the cracks. The solid curves are with the present method and the circles with FEM.*

In the present thesis the numerical examples and comparisons with FEM calculations are foremost given to confirm the accuracy of the methods. The following two examples

from papers C and D are even so containing some interesting information. In the first figure 4.1 the change in impedance when scanning perpendicular over the center of rectangular cracks with five different lengths 10 mm, 8 mm, 4 mm, 2 mm and 1 mm are shown. The cracks breaks a plane surface of titanium, they are 0.66 mm high and the frequency of the current is 1 MHz. There is five different crack lengths, but there are only four different curves. All cracks that are longer than 8 mm give the same change in impedance. This imply that the change in impedance due to a rectangular crack can be calculated by use of the method in paper B for a strip-like crack when the probe is not to close to the edge of the crack (a distance of 4 mm from the edge is enough in example 4.1). The circles in the figure which agrees very well with the curves are finite element calculations. Good agreement with FEM is found for all methods in the present thesis. The change in impedance is presented in the impedance plane which is common in eddy current applications. Here the imaginary part corresponds to change of the reactance while the real part corresponds to change of the resistance. All of the curves are coinciding at the origin where the probe position is far away from the position of the crack. The signal is increasing when the probe is approaching the crack.

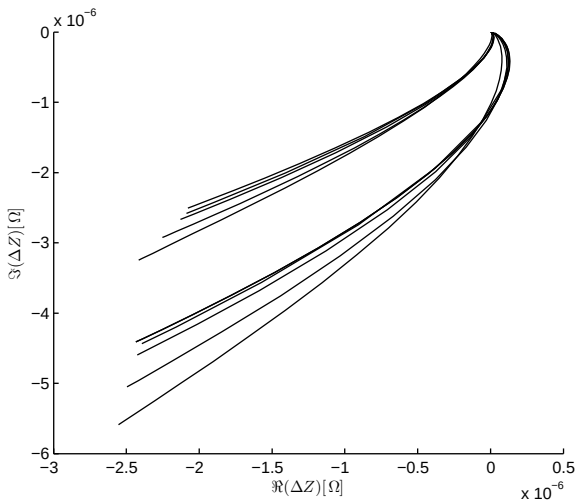

Figure 4.2: *The real versus the imaginary part of* ΔZ *during a surface scan. The lengths of the cracks are* 2 mm, 4 mm *(starting from the top). The scanning is in the* ϕ *direction over the center of the cracks. The radii of the cylindrical hole are* 1.5 mm, 2.5 mm, 5 mm, 7.5 mm *and* ∞ mm, *where the amplitude is decreasing with increasing radii.*

Figure 4.2 is from paper D and shows the change in impedance when scanning inside cylindrical holes with four different radii, 1.5 mm, 2.5 mm, 5 mm and 7.5 mm. Again the material is titanium, the height of the cracks is 0.66 mm and the applied frequency 1 MHz. The fifth curve shows the result for the same scan, but when the surface is a plane. The model of a crack inside the material with plane surface could be used as a

good approximation for the crack below the cylindrical surface when the radius is large (larger than $r_c = 7.5\,\text{mm}$ in this case). This is an important observation in the intention of making computational efficient simulations, especially since the effectiveness of the integral equation method presented in paper D is decreasing when the radius of the cylinder is increased. A larger number of cylindrical basis functions which are used in the expansions of the incoming field and the reflected part of the Green's tensor is needed for a cylinder of larger radius.

5 Summary of appended papers

5.1 Paper A

A 2D model of the eddy current interaction problem that consists of an inhomogeneity in a conductive half space is presented. The applied analytical method of solution is the transition (T) matrix method. This involves use of the free space Green's function to generate a system of boundary integral relations. In this way, it is easy to identify the contributions to the total solution from each different scattering surface. The different parts are separated also in the computation of the impedance. This leads to low cost simulations in terms of computation time and qualify the method to be used to obtain probability of detection (POD) curves. The model is compared with a Finite Element (FE) model and numerical examples for the case with a cylindrical inhomogeneity are given. This method is foremost suitable to subsurface defects and not to surface-breaking once, even though it is possible to be near the surface. The efficiency of the method and its building block characteristics enable applications where several scatterers are involved.

5.2 Paper B

An integral equation method to the nondestructive evaluation problem for a flat, infinitely long, tilted, surface-breaking crack in a conducting half-space is presented. The method involves use of the half-space Green's function and the Bowler potential. This potential describes the jump in the electric field over the crack and is expanded in basis functions related to the Chebyshev polynomials, being a more analytical approach than the commonly used boundary element method (BEM). A similar approach was used by Bövik and Boström [2] to model a subsurface crack in an elastodynamic field problem. In the method the scatterer defines a transformation operator to be applied on the incoming field. This is practical in simulations of the eddy current inspection where this operator just has to be generated once and not for every position of the probe. The numerical calculations of the change in impedance due to the crack are compared with a Finite Element (FE) model of the problem and good agreement is found. The infinite length of the defect is one of the reasons for the efficiency of the method, even so the model can be used as an good approximation for long enough rectangular cracks.

5.3 Paper C

The eddy-current nondestructive evaluation problem for a flat, rectangular, tilted, surface-breaking crack in a conducting half-space is solved using a similar method as in paper B. The obvious difference of the rectangular crack compared to the infinitely long crack is the presence of corners and two more edges. The key point is to expand the Bowler potential, i.e. the difference in electric potential over the crack, in basis functions who have the correct behavior along the crack edges. Here two different sets of basis functions related to the Chebyshev polynomials are used. The way of discretization in this method leads to a formulation where the scattering is defined by a scattering matrix, independent of the incoming field. This is an advantage of the method and being a more analytical approach than the commonly used boundary element method suggests that it can be expected to be more numerically effective. Numerical examples are given and compared with Finite Element calculations and good agreement is found.

5.4 Paper D

An integral equation method for solving the eddy-current nondestructive evaluation problem for a flat, rectangular, crack close to a cylindrical hole in a conducting material is presented. The method involves expanding the Green's tensor, the incoming field and the jump in electric potential over the crack in suitable basis functions. Here plane waves, cylindrical waves and basis functions related to the Chebyshev polynomials are used. The way of discretization in this method leads to a formulation where the scattering is defined by a scattering matrix, independent of the incoming field. This is an advantage in the simulations where the scattering matrix does not have to be recalculated for every probe position. The numerical calculations are straightforward and examples are given and compared with Finite Element calculations. The basis functions used in this paper to model a subsurface crack are different from those used in paper B and C to model a surface-breaking crack.

6 Concluding remarks

In this thesis methods of solution for elastic wave scattering have been used to solve the eddy current scattering problem. All of the methods is based on a Green's function technique and integral representations and are restricted to problems in homogeneous and isotropic media. The T matrix method described in paper A and the integral equation methods described in paper B, C and D have all shown to be applicable methods of solution for the eddy current interaction problem. The advantage compared to numerical methods such as FEM or BEM is the computational efficiency. The computations made with the T matrix method were carried out 10 to 50 times faster than the corresponding finite element computations. The simulations done with the integral equation methods in papers B, C and D were about 10 times faster than the FEM simulations made for comparisons. The more probe positions used in the simulations the more beneficial

becomes the methods compared with FEM. These numbers can most likely be greatly improved by optimization of the implementations.

The T matrix method has the great advantage of being a building block method, meaning that several T matrices describing different scatterers can be easily put together into a total T matrix which generates the total scattered field. The method can also be used together with a finite element method solution approach to manage complex scattering geometries. On the other hand, it is preferable to use other analytical methods to obtain different scattering geometries when possible. An ellipsoid is an example of such a geometry and by use of the method described in [20] the geometry could be altered in other ways.

The integral equation methods are efficient methods using discretizations in appropriate basis functions. The choice of correct basis functions is the key point for these methods to be successful. There are two different sets of basis functions, one to model the surface-breaking crack in paper B and C and another to model the near surface crack in paper D. The characteristics of these basis functions are very similar to the characteristics of the involved fields leading to fast convergence. On the other hand these special properties of the basis functions are also making them incapable to be applied to a crack of general geometry for example. Neither can the basis functions used on the surface-breaking crack be used to model a subsurface crack or vice versa. The Chebyshev related basis used in paper D on the surface of a subsurface rectangular crack parallel to the axis of the cylinder can also be used on a radial crack in the same geometry. To model a surface breaking radial crack the same basis as in paper B and C can also be used here. The radial crack is more suited to break the surface due to the possibilities to express the G_{zz} component of the Green's tensor as a suitable expansion. Another common crack geometry where there exists suitable basis functions to discretize the integral equation is the half-circular crack. These basis functions are related to the Legendre polynomials.

A useful extension of the work would be to reformulate the model of electrical contact over the crack such that a model of a crack with a small width is obtained.

References

[1] B. Auld and J. Moulder. Review of advances in quatitative eddy current nondestructive evaluation. *J. Nondestruct. Eval.* **18** (1999), 3–36.

[2] P. Bövik and A. Boström. A model of ultrasonic nondestructive testing for internal and subsurface cracks. *J. Acoust. Soc. Am.* **102** (1997), 2723–2733.

[3] J. Bowler. Eddy current interaction with an ideal crack, Part I: The forward problem. *J. Appl. Phys.* **75** (1994), 8128–8137.

[4] S. Burke and T. Theodoulidis. Impedance of a horizontal coil in a borhole: model for eddy-current bolthole probes. *J. Phys. D: Appl. Phys* **37** (2004), 485–494.

[5] C. Dodd and W. Deeds. Analytical solutions to eddy-current probe-coil problems. *J. Appl. Phys.* **39**.6 (1968), 2829–2838.

[6] N. Harfield and J. Bowler. A geometrical theory for eddy-current non-destructive evaluation. *Proc. Roy. Soc. Lond. A* **453** (1997), 1121–1152.

[7] N. Harfield and J. Bowler. Analysis of eddy-current interaction with a surface-breaking crack. *J. Appl. Phys.* **76** (1994), 4853–4856.

[8] F. Jensen, S. Mahaut, P. Calmon, and C Poidevin. "Simulation based POD evaluation of NDI techniques". *10th European Conference on Nondestructive Testing.* Moscow, 2010.

[9] A. Karlsson. Scattering from inhomogeneities in layered structures. *J. Acoust. Soc. Am.* **71** (1981), 1083–1092.

[10] A. Krawczyk and T. J.A. *Numerical modelling of eddy currents.* Oxford University Press Inc., 1993.

[11] G. Kristensson. "Electromagnetic scattering from a buried three-dimensional inhomogeneity in a lossy ground". *Electromagnetic Theory Symposium URSI.* Munich, 1980.

[12] G. Kristensson and S. Ström. Scattering from buried inhomogeneities - a general three-dimensional formalism. *J. Acoust. Soc. Am.* **64** (1978), 917–936.

[13] L. Larsson. Integral equation method for evaluation of eddy-current impedance of a tilted, rectangular, surface-breaking crack. *To be submited for international publication.* (2014).

[14] L. Larsson and A. Boström. Integral equation method for evaluation of eddy-current impedance of a rectangular, near surface crack inside a cylindrical hole. *To be submited for international publication.* (2014).

[15] L. Larsson, A. Boström, P. Bövik, and H. Wirdelius. Integral equation method for eddy current nondestructive evaluation of a tilted, surface-breaking crack. *J. Appl. Phys.* **114** (2013), 194504 –194504–6.

[16] L. Larsson and A. Rosell. "The T matrix method for a 2D eddy current interaction problem". *AIP Conf. proc. Reveiw of progress in quantitative nondestructive evaluation.* Vol. 1430. Burlington, Vermont, 2012, pp. 316–323.

[17] A. Lewis, D. Michael, M. Lugg, and R. Collins. Thin-skin electromagnetic fields around surface-breaking cracks in metals. *J. Appl. Phys.* **64** (1988), 3777–3784.

[18] J. Maxwell. A dynamical theory of the electromagnetic field. *Phil. Trans. Royal Soc. London* **155** (1865), 459–512.

[19] I. N. *Numerical modeling for electromagnetic non-destructive evaluation. Engineering NDE.* London: Chapman & Hall, 1995.

[20] D. Prémel. Computation of a quasi-static field induced by two long straight parallel wires in a conductor with a rough surface. *J. Phys. D: Appl. Phys.* **41** (2008).

[21] A. Rosell and G. Persson. Model based capability assessment of an automated eddy current inspection procedure on flat surfaces. *Res. Nondestr. Eval.* **24** (2013), 154–176.

[22] T. Theodoulidis. Developments in efficiently modelling eddy current testing of narrow cracks. *NDT & E International* **43** (2010), 591–598.

[23] H. Wirdelius and G. Persson. Simulation based validation of an ultrasonic inspection procedure. *Int. J. Fracture* **41** (2012), 23–29.

[24] L. Yu, J. Bowler, and T. Theodoulidis. An analytical model of a ferrite-cored inductor used as an eddy current probe. *J. Appl. Phys* **111** (2012), 103907–1–103907–10.